ANL/NDM--97

DE87 005541

ANL/NDM-97

THE FISSION CROSS SECTIONS OF ^{230}Th, ^{232}Th, ^{233}U, ^{234}U, ^{236}U, ^{238}U, ^{237}Np, ^{239}Pu AND ^{242}Pu RELATIVE ^{235}U AT 14.74 MEV NEUTRON ENERGY

by

J. W. Meadows

December, 1986

Keywords:

DISCLAIMER

---

*This work supported by the U. S. Department of Energy, Nuclear Energy Programs under contract W-31-109-Eng-38.

Applied Physics Division
Argonne National Laboratory
9700 S. Cass Avenue
Argonne, Illinois 60439
U. S. A.

NUCLEAR DATA AND MEASUREMENTS SERIES

The Nuclear Data and Measurements Series presents results of studies in the field of microscopic nuclear data. The primary objective is the dissemination of information in the comprehensive form required for nuclear technology applications. This Series is devoted to: a) measured microscopic nuclear parameters, b) experimental techniques and facilities employed in measurements, c) the analysis, correlation and interpretation of nuclear data, and d) the evaluation of nuclear data. Contributions to this Series are reviewed to assure technical competence and, unless otherwise stated, the contents can be formally referenced. This Series does not supplant formal journal publication but it does provide the more extensive information required for technological applications (e.g., tabulated numerical data) in a timely manner.

Copies on microfiche can be obtained by contacting:

National Technical Information Service
U.S. Department of Commerce
5285 Port Royal Road
Springfield, Virginia 22161
U.S.A.

INFORMATION ABOUT OTHER ISSUES IN THE ANL/NDM SERIES

A list of titles and authors for reports ANL/NDM-1 through ANL/NDM-50 can be obtained by referring to any report of this Series numbered ANL/NDM-51 through ANL/NDM-76. Requests for a complete list of titles or for copies of previous reports should be directed to:

Section Secretary
Applied Nuclear Physics Section
Applied Physics Division
Building 316
Argonne National Laboratory
9700 South Cass Avenue
Argonne, Illinois 60439
U.S.A.

ANL/NDM-51 A. Smith, P. Guenther, D. Smith and J. Whalen, *Measured and Evaluated Cross Sections of Elemental Bismuth*, April 1980.

ANL/NDM-52 P. Guenther, A. Smith and J. Whalen, *Neutron Total and Scattering Cross Sections of ^{6}Li in the Few-MeV Region*, February 1980.

ANL/NDM-53 James W. Meadows and Donald L. Smith, *Neutron-source Investigations in Support of the Cross-section Program at the Argonne Fast-neutron Generator*, May 1980.

ANL/NDM-54 A.B. Smith, P.T. Guenther and J.F. Whalen, *The Nonelastic-scattering Cross Sections of Elemental Nickel*, June 1980.

ANL/NDM-55 M.M. Bretscher and D.L. Smith, *Thermal-neutron Calibration of a Tritium Extraction Facility using the* $^{6}Li(n,t)^{4}He/Au(n,\gamma)^{198}Au$ *Cross-section Ratio for Standardization*, August 1980.

ANL/NDM-56 P.T. Guenther, A.B. Smith and J.F. Whalen, *Fast-neutron Interaction with* ^{182}W, ^{184}W *and* ^{186}W, December 1980.

ANL/NDM-57 Peter T. Guenther, Alan B. Smith and James F. Whalen, *The Total, Elastic- and Inelastic-scattering Fast-neutron Cross Sections of Natural Chromium*, January 1981.

ANL/NDM-58 W.P. Poenitz, *Review of Measurement Techniques for the Neutron-capture Process*, August 1981.

ANL/NDM-59 Wolfgang P. Poenitz, *Review of the Importance of the Neutron-capture Process in Fission Reactors*, July 1981.

ANL/NDM-60 James W. Meadows and Donald L. Smith, *Gamma-ray Detector Calibration Methods Utilized in the Argonne FNG Group Activation Cross-section Measurement Program*, April 1984.

ANL/NDM-61 Carl Budtz-Joergensen, Peter T. Guenther, Alan B. Smith and James F. Whalen, *Fast-neutron Total and Scattering Cross Sections of* ^{58}Ni, September 1981.

ANL/NDM-62 Donald L. Smith, *Covariance Matrices and Applications to the Field of Nuclear Data*, November 1981.

ANL/NDM-63 Alan B. Smith and Peter T. Guenther, *On Neutron Inelastic-scattering Cross Sections of* ^{232}Th, ^{233}U, ^{235}U, ^{238}U, ^{239}U *and* ^{239}Pu *and* ^{240}Pu, January 1982.

ANL/NDM-64 James W. Meadows and Carl Budtz-Joergensen, *The Fission-fragment Angular Distributions and Total Kinetic Energies for $^{235}U(n,f)$ from 0.18 to 8.83 MeV*, January 1982.

ANL/NDM-65 Alan B. Smith and Peter T. Guenther, *Note on the Elastic Scattering of Several-MeV Neutrons from Elemental Calcium*, March 1982.

ANL/NDM-66 Alan B. Smith and Peter T. Guenther, *Fast-neutron Scattering Cross Sections of Elemental Silver*, May 1982.

ANL/NDM-67 Donald L. Smith, *Non-evaluation Applications for Covariance Matrices*, July 1982.

ANL/NDM-68 Alan B. Smith, Peter T. Guenther and James F. Whalen, *Fast-neutron Total and Scattering Cross Sections of ^{103}Rh*, July 1982.

ANL/NDM-69 Alan B. Smith and Peter T. Guenther, *Fast-neutron Scattering Cross Sections of Elemental Zirconium*, December 1982.

ANL/NDM-70 Alan B. Smith, Peter T. Guenther and James F. Whalen, *Fast-neutron Total and Scattering Cross Sections of Niobium*, July 1982.

ANL/NDM-71 Alan B. Smith, Peter T. Guenther and James F. Whalen, *Fast-neutron Total and Scattering Cross Sections of Elemental Palladium*, June 1982.

ANL/NDM-72 Alan B. Smith and Peter T. Guenther, *Fast-neutron Scattering from Elemental Cadmium*, July 1982.

ANL/NDM-73 C. Budtz-Joergensen, Peter T. Guenther and Alan B. Smith, *Fast-neutron Elastic-scattering Cross Sections of Elemental Tin*, July 1982.

ANL/NDM-74 Wolfgang Poenitz, Alan B. Smith and Robert Howerton, *Evaluation of the ^{238}U Neutron Total Cross Section*, December 1982.

ANL/NDM-75 A.B. Smith, P.T. Guenther and J.F. Whalen, *Neutron Total and Scattering Cross Sections of Elemental Antimony*, September 1982.

ANL/NDM-76 Alan B. Smith and Peter T. Guenther, *Scattering of Fast Neutrons from Elemental Molybdenum*, November 1982.

ANL/NDM-77 Donald L. Smith, *A Least-squares Method for Deriving Reaction Differential Cross Section Information from Measurements Performed in Diverse Neutron Fields*, November 1982.

ANL/NDM-78 A.B. Smith, P.T. Guenther and J.F. Whalen, *Fast-neutron Total and Elastic-scattering Cross Sections of Elemental Indium*, November 1982.

ANL/NDM-79 C. Budtz-Joergensen, P. Guenther, A. Smith and J. Whalen, *Few-MeV Neutrons Incident on Yttrium*, June 1983.

ANL/NDM-80 W.P. Poenitz and J.F. Whalen, *Neutron Total Cross Section Measurements in the Energy Region from 47 keV to 20 MeV*, July 1983.

ANL/NDM-81 D.L. Smith and P.T. Guenther, *Covariances for Neutron Cross Sections Calculated Using a Regional Model Based on Elemental-model Fits to Experimental Data*, November 1983.

ANL/NDM-82 D.L. Smith, *Reaction Differential Cross Sections from the Least-squares Unfolding of Ratio Data Measured in Diverse Neutrons Fields*, January 1984.

ANL/NDM-83 J.W. Meadows, *The Fission Cross Sections of Some Thorium, Uranium, Neptunium and Plutonium Isotopes Relative to* ^{235}U, October 1983.

ANL/NDM-84 W.P. Poenitz and J.W. Meadows, *^{235}U and ^{239}Pu Sample-mass Determinations and Intercomparisons*, November 1983.

ANL/NDM-85 D.L. Smith, J.W. Meadows and I. Kanno, *Measurement of the $^{51}V(n,p)^{51}Ti$ Reaction Cross Section from Threshold to 9.3 MeV*, June 1984.

ANL/NDM-86 I. Kanno, J.W. Meadows and D.L. Smith, *Energy-differential Cross-section Measurement for the $^{51}V(n,\alpha)^{48}Sc$ Reaction*, July 1984.

ANL/NDM-87 D.L. Smith, J.W. Meadows, M.M. Bretscher and S.A. Cox, *Cross-section Measurement for the $^{7}Li(n,n't)^{4}He$ Reaction at 14.74 MeV*, September 1984.

ANL/NDM-88 A.B. Smith, D.L. Smith and R.J. Howerton, *An Evaluated Nuclear Data File for Niobium*, March 1985.

ANL/NDM-89 Bernard P. Evain, Donald L. Smith and Paul Lucchese, *Compilation and Evaluation of 14-MeV Neutron-activation Cross Sections for Nuclear Technology Applications: Set I*, April 1985.

ANL/NDM-90 D.L. Smith, J.W. Meadows and P.T. Guenther, *Fast-neutron-spectrum Measurements for the Thick-target $^{9}Be(d,n)^{10}b$ Reaction at E_d = 7 MeV*, April 1985.

ANL/NDM-91 A.B. Smith, P.T. Guenther and R.D. Lawson, *On the Energy Dependence of the Optical Model of Neutron Scattering from Niobium*, May 1985.

ANL/NDM-92 Donald L. Smith, *Nuclear Data Uncertainties (Vol.-I): Basic Concepts of Probability*, April 1986.

ANL/NDM-93 D.L. Smith, J.W. Meadows and M.M. Bretscher, *Integral Cross-section Measurements for* $^{7}Li(n,n't)^{4}He$, $^{27}Al(n,p)^{27}Mg$, $^{27}Al(n,\alpha)^{24}Na$, $^{58}Ni(n,p)^{58}Co$ *and* $^{60}Ni(n,p)^{60}Co$ *Relative to* ^{238}U *Neutron Fission in the Thick-target* $^{9}Be(d,n)^{10}B$ *Spectrum at* E_d = 7 *MeV*, October 1985.

ANL/NDM-94 A.B. Smith, D.L. Smith, P. Rousset, R.D. Lawson and R.J. Howerton, *Evaluated Neutronic Data File for Yttrium*, January 1986.

ANL/NDM-95 Donald L. Smith and James W. Meadows, *A Facility for High-intensity Neutron Irradiations Using Thick-target Sources at the Argonne Fast-neutron Generator*, May 1986.

ANL/NDM-96 M. Sugimoto, A.B. Smith and P.T. Guenther, *Ratio of the Prompt-Fission-Neutron Spectrum of Plutonium 239 to that of Uranium 235*, September 1986.

TABLE OF CONTENTS

ANL/NDM-97

The Fission Cross Sections of ^{230}Th, ^{232}Th, ^{233}U, ^{234}U, ^{236}U, ^{238}U, ^{237}Np, ^{239}Pu and ^{242}Pu Relative ^{235}U at 14.74 MeV Neutron Energy

by

J. W. Meadows

December, 1986

Applied Physics Division

Argonne National Laboratory

Argonne, Illinois 60439

ABSTRACT

The measurement of the fission cross section ratios of nine isotopes relative to ^{235}U at an average neutron energy of 14.74 MeV is described with particular attention to the determination of corrections and to sources of error. The results are compared to ENDF/B-V and to other measurements of the past decade. The ratio of the neutron induced fission cross section for these isotopes to the fission cross section for ^{235}U are: ^{230}Th - 0.290 ± 1.9%; ^{232}Th - 0.191 ± 1.9%; ^{233}U - 1.132 ± 0.7%; ^{234}U - 0.998 ± 1.0%; ^{236}U - 0.791 ± 1.1%; ^{238}U - 0.587 ± 1.1%; ^{237}Np - 1.060 ± 1.4%; ^{239}Pu - 1.152 ± 1.1%; ^{242}Pu - 0.967 ± 1.0%.

---

*This work supported by the U. S. Department of Energy, Nuclear Energy Programs under Contract W-31-109-Eng-38.

INTRODUCTION

Accurate values of the ratios of fission cross sections are important for neutronic calculations, as spectral indices in the measurement of neutron spectra and as a check on the reliability of cross section measurements. Now, with the improved accuracy of the ^{235}U fission cross section and its use as a reference cross section, ratios relative to ^{235}U become useful cross section measurements in themselves.

The 14.7 MeV energy point is near the upper limit of the fission neutron spectrum and thus is not of much direct interest for fission reactors, but it is a very important energy for fusion applications. Furthermore, it provides a convenient normalization point for many broad spectrum cross section measurements. Unfortunately, this point is not well located for the normalization of fission cross sections since the threshold for the (n,2nf) reactions are in this region and both fission cross sections and cross section ratios may show a significant energy dependence. However the low cost and wide distribution of 14 MeV generators is another consideration. When measurements are being made near the limit of accuracy it becomes difficult to ensure that one or two measurements, no matter how carefully carried out, do not contain undetected systematic errors. The wide distribution of the 14 MeV generators at least provides the opportunity for a number of independent measurements which, in the aggregate, can provide some insurance against such errors.

For several years there has been an on-going fission cross section ratio program at the Argonne Fast Neutron Generator and results have been reported for 10 isotopes in the energy range 0.1-10 MeV (1-11). This report describes measurements at 14.74 MeV using many of the samples that were originally prepared for the lower energy measurements. The basic experimental method was the same but the characteristics of a 14 MeV neutron source and the equipment available at our particular facility required a number of changes. Secondary experiments designed to determine or test some of the corrections are described in detail. Although many of

the experimental procedures are described in other publications enough detail is included in this report to allow it to be read without reference to the earlier work.

II. THE EXPERIMENTAL METHOD

In the ideal measurement thin deposits of a material whose principal isotope is r and of a material whose principal isotope is x are placed in identical neutron beams and their true fission rates are measured. The true fission rate ratio of the two samples is related to the ratio of the fission cross sections by

$$\frac{\mathcal{F}_1}{\mathcal{F}_2} = \frac{N_1\,\sigma_x}{N_2\,\sigma_r}\,\frac{\sum_i P_{1i}\,(\sigma_i/\sigma_x)}{\sum_j P_{2j}\,(\sigma_j/\sigma_r)} \qquad (1)$$

where

- x is the principal isotope of sample 1.
- r is the reference isotope and is the principal isotope in sample 2, in this case ^{235}U.
- i refers to the isotopes in sample 1.
- j refers to the isotopes in sample 2.
- $\mathcal{F}$ is the true fission rate.
- N is the number of atoms of the fissionable element in a sample.
- σ the fission cross section.
- P is the isotopic mole fraction.

The sum terms may be considered to be a correction factor that corrects for the presence of isotopes other than x and r.

The actual experimental arrangement is illustrated in Fig. 1. Thin layers of fissionable materials were deposited on thin plates and placed back-to-back in a low-mass double ionization chamber and oriented perpen-

dicular to a neutron beam where their relative fission rates were measured. The ratio of the observed fission rates were converted to the ratio of the true fission rates by applying a number of correction factors as follows:

$$(2) \qquad \frac{\mathcal{F}_1}{\mathcal{F}_2} = \left[\frac{F_{1f} - B_{1f} + \beta_{1f} + c}{F_{2b} - B_{2b} + \beta_{2b} + c}\right] \frac{G_f\ T_f\ L_{1f}\ S_{1f}}{G_b\ L_{2b}\ S_{2b}}$$

where

- b refers to the sample in the 180 degree position , i.e., facing the neutron source.
- f refers to the sample in the 0 degree position.
- c is the coincidence correction.
- F is the observed fission rate.
- B is the room return correction.
- S is the factor to correct for prompt neutron scattering.
- β is the correction for those fission pulses that lie below the discriminator level.
- L is the correction for sample thickness, momentum transferr and fragment angular distribution.
- G is the geometry factor.
- T_f is the transmission factor for the deposit support plates. T_b is always 1.0.

Equation (2) is written explicitly for the case where sample 1 is in the zero degree position (i.e., facing away from the neutron source) and a similar expression can be written for sample 2 in that position. Measurements were made in these two orientations and averaged. If G_f/G_b, T_f and the ratios of the other position dependent correction factors are very near to 1.0, then the G and T terms will cancel to first order and the correction terms may be replaced by average values. In this experimental arrangement higher-order terms are generally negligible so

equations (1) and (2) can be combined to give

$$(3) \qquad \overline{\left[\frac{C_1}{C_2}\right]} \frac{\bar{L}_1 \bar{S}_1}{\bar{L}_2 \bar{S}_2} = \frac{N_1 \sigma_x \sum_i P_{1i}(\sigma_i/\sigma_x)}{N_2 \sigma_r \sum_j P_{2j}(\sigma_j/\sigma_r)}$$

where

$$C = F - B + \beta + c$$

The bar over a term indicates an average over the two sample orientations. There are additional advantages to this procedure. The correction for momentum which is included in L usually vanishes to first order (see Section V. C.) and the position dependence of S on the orientation of the samples is removed.

III. APPARATUS

A. Neutron Source.

Deuterons were accelerated by a Texas Nuclear Generator (12) with 150 keV on the terminal. The deuteron beam was sent through a magnet which deflected the D^+ beam about 10 degree, sufficient to separate it from the D_2^+ beam. The D^+ beam impinged on a titantium tritide target to produce neutrons by means of the $T(D,n)^4He$ reaction. These targets were obtained commercially (13) and consisted of a thin layer of titantium on a 0.13 mm thick copper plate containing about 1 Ci/cm^2 of tritium when fresh. The targets were mounted in the air-cooled assembly shown in Fig. 1. For the present measurements the accelerator was usually operated in the slow pulsed mode with a 5 μsec wide pulse and a 21 μsec period. Typical beam currents at the tritium target were about 25 μamps. The energy profile of neutrons incident on a 2.54 cm dia. detector 6.5 cm from the source is shown in Fig. 2. This was calculated assuming that the titantium layer was thicker than the range of a 150 keV deuteron and that the tritium was uniformally distributed through the titantium layer.

B. Fission Detector and Electronics.

The basic fission detector and electronics were very similar to those used for the earlier measurements below 10 MeV (1-11). However the 14 MeV generator was not capable of nanosecond pulsing and no multiparameter analyzer was avaliable at the facility, so some changes were required.

The fission detector, shown schematically in Fig. 1, was unchanged. It was a low mass double ionization chamber with fissionable deposits on both sides of a common cathode. It was made from a steel specimen container with 0.25 mm thick walls and a friction fit lid and was operated as a flow counter using a mixture of 90 % argon-10 % methane instead of the usual pure methane. This mixture gave an adequate electron mobility and reduced the number of proton recoils which gave an undesirable background. The cathode-anode separation was $\simeq$ 0.6 cm and the voltage gradient was $\simeq$ 650 V/cm.

A simplified diagram of the electronic set-up is shown in Fig. 3. The fast rise of the current pulse in parallel plate ionization chambers was used to provide good timing characteristics and to maintain good separation between the alphas and fissions at very high alpha rates. A good discussion of the principals of this type of ion-chamber operation is given in ref. (14). Signals from the ion chamber anode went to a charge sensitive preamplifier. The output went to a double differentiating amplifier where the first differentiation was accomplished by a shorted 93 Ω coaxial cable to produce the current pulse, and the second was produced by the 10 nanosecond amplifier time constant to form an output pulse with a total width $\simeq$ 50 nanosecond and an area proportional to the number of ion pairs created in the ion chamber. The amplifier output was divided with part going to constant fraction discriminator which initiated a 60 nanosecond gate signal and provided the START signal for the time to amplitude converter (TAC). Another part went to a fast linear gate and stretcher, which was controlled by the gate signal, whose output was proportional to the area of the input pulse. Since the alphas were

removed by the gate before the pulses were stretched alpha pile-up was kept to minimium. Data was stored in a four group multichannel analyzer. Group 1 contained those events that were accompanied by a routing signal from detector 1 while group 2 contained those from detector 2. Those events that were not accompanied by any routing signals were stored in group 0 while those events that were accompanied by both signals were stored in group 3. This information was used for the coincidence correction defined in Section II. A typical pulse height spectrum is shown in Fig. 4. As shown in Fig. 3, the system could also produce a time distribution of the fission events relative to the accelerator beam pulse but the time and pulse-height distributions could not be recorded simultaneously. A typical time spectrum for ^{235}U is shown in Fig. 5. These spectra were used to determine the number of fissions produced by low energy room return neutrons and they are discussed further in Section V. B.

C. Alpha Counter.

The alpha decay rates of all the samples were determined in a low-geometry counter constructed to tolerances of 0.0025 mm. Alphas were detected by a silicon detector placed behind a 1.270 cm diameter aperture. Samples were mounted on a holder that could be placed in several positions beginning at 4.57 cm from the aperture while subsequent positions increased the distance by multiples of 5.08 cm. Except for the aperture this was the same detector used in the earlier measurements (1-11). The new aperture had a smaller "lip" and did not require the correction discussed in ref. (15). The geometry factors were calculated by Monte Carlo (16) intergration and also by a series expansion (17). Alpha spectra were recorded in a 1024 channel analyzer, and counts were obtained by intergrating over the appropriate alpha energy range.

IV. SAMPLE PREPARATION AND ASSAY

The fissionable samples and their isotopic composition are listed in

Tables I, II and III. Additional sample information, including the weights and specific activities, are listed in Table IV. All the samples were thin deposits, a nominal 2.54 cm in diameter, on 0.25 mm thick stainless steel plates, 0.13 mm thick molybdenum plates or on 0.13 mm thick platinium plates. The thorium and most of the uranium samples were prepared by molecular plating following a procedure developed by Parker et al. (18). The neptunium and plutonium samples were deposited using a method described by Ko (19). Two of the ^{235}U deposits were prepared by vacuumn evaporation of UF_4.

When this program of fission ratio measurements was begun (about 1968) the status of the half-life data for the isotopes involved was poor so every effort was made to measure N, the number of atoms in the sample, or N_1/N_2, the ratio of sample atoms, by methods which did not involve half-lives. Fortunately this situation has changed greatly in the past decade and there now exists an impressive body of more accurate data for the longer-lived actinides and errors associated with the alpha half-lives are now relatively minor parts of the total error in the fission cross section ratios. In the present work many of the uranium ratio measurements still do not depend on half-life information since the principal alpha emitter in each sample was the same isotope (i.e., ^{234}U for the ratio measurement with U-234-5/U-235 5-2). Also N_1/N_2 for several pairs of samples was obtained by measuring their relative thermal fission rates. This procedure was described and up-dated in ref. (11) and those results were used in the present measurements. The samples involved are indicated in Table IX.

The weights of all samples, listed in Table IV, were based on specific alpha activities calculated from the isotopic analyses and the half-lives given in Table V. The calculated specific activity, also given in Table IV, includes only those alphas accepted by the analyzer window. Thus the short-lived isotopes and decay products, which have higher alpha energies and which were present in uncertain amounts, were not counted.

Many of these samples were used in the earlier measurements and the present weights may be compared with those given in ref. (11). In making this comparison it must be remembered that the present weights are based on new alpha counts, in a counter with a different aperture, using revised half-life information and, in some cases, revised isotopic analyses. On the whole the agreement is quite good.

Only one of the ^{238}U samples (U-238 8-2) dated from an earlier measurement. It was a ^{238}U - ^{235}U mixture that was paired with U-235 5-2 and N_1/N_2 was obtained by measuring their relative thermal fission rates. The other samples were representatives of two ^{233}U - ^{238}U mixtures, a ^{234}U - ^{238}U mixture and a thick ^{238}U sample of very high isotopic purity. The activity of the latter material (238-60) was almost entirely due to ^{238}U and was just large enough to allow a reasonably accurate alpha count with a geometry factor of about 220. The part of the 0.6 ppm impurity that was ^{234}U was eliminated by the analyzer window. If there was any ^{235}U present at the level indicated by the analyses it would have had a negligible effect on the alpha and fission rates.

Two of these samples (U-235 SST-5 and U-235 5-2) were used in a sample-mass intercomparison involving samples from several laboratories (15). Since these measurements were reported, additional isotopic analysis have become available. These caused minor changes for the 5-2 sample and resulted in better agreement between the calculated specific activity, the result of isotopic dilution measurements and the sample intercomparison. The effect on the SST-5 sample was a little larger, but it also produced better agreement with the intercomparison.

V. CORRECTIONS TO THE DATA.

A. Prompt Scattered Neutrons.

Neutrons scattered by material in the immediate vicinity of the neutron source and the fission deposit are most effective in producing fissions. The amount of scattering from the structures shown in Fig. 1 was calculated using the Monte Carlo program CYSCAT which is described in

ref. (23). This program permits the inclusion of the angle and energy distribution of the source neutrons as well as energy and angle dependent scattering cross sections. It only considers a single scattering but this should not be a serious fault; the structures involved are light so the multiple scattering contribution should be small. A more serious simplification lies in the handling of inelastic scattering wnich is the principal contributor to the correction to the fission cross section ratio. Direct interactions were ignored. All neutrons from the (n,n') and (n,2n) reactions were assumed to be isotropic and to have and energy distributions of the form

$$N(E) = K\, E\, e^{(2\, a(E^{*} - E_s - E))^{1/2}} \tag{4}$$

where K is a normalization constant, E^{*} is the nuclear excitation energy, E_s is the neutron separation energy from the compound nucleus and E is the energy of the emitted neutron. Fission from neutrons scattered from these structures ranged from $\simeq$ 4 % for Th^{232} to $\simeq$ 6 % for ^{235}U.

Fissions were also produced by neutrons scattered from more distant objects such as the floor, walls, air, etc., but the correction should be negligible because of the small solid angle of the deposit relative to the point of scattering. This assumption was tested by measuring the ^{238}U fission rate as a function of D, the source-deposit distance. If scattering occurs, on the average, at distances much larger than D, then the scattered neutron fission contribution should be insensitive to D while the number of fissions due to neutrons coming directly from the source should be proportional to $1/D^2$.

The fission counter, containing a high purity ^{238}U deposit (U-238-60), was placed at 0 degree with respect to the deuteron beam. The neutron source strength was monitored by a long counter positioned at right angles to the beam line and at a distance of about 10 meters. Measurements were made for several values of D. The fission counts were normalized to the long counter and corrected for scattering from the source and detector structures. The results were fitted by

$$CG = a + b\,G$$

where C is the normalized fission count and G is the fission-deposit-neutron-source geometry factor. G is proportional to D^2 when D is large, but it was necessary to use G because of the departure from a D^2 dependence at small D. If all the neutrons that produced fissions came directly from the source, b would be 0. The result, normalized to 1.0 at G=0, was

$$CG = 1.0 - (1.0 \pm 2.2) \times 10^{-5}.G$$

Most of the ratio measurements were made with $G \simeq 125$, so the estimated prompt scattering from distant sources into the ^{238}U detector was - 0.1 ± 0.2 %. No correction was made for this effect.

B. Room Return.

In this report the term "room return" refers to those neutrons which have been degraded to such a low energy by multiple scattering that they showed no significant time dependence over periods $\geq$ 20 μsec. Typically these neutrons produced about 5 % of the total fissions in the ^{235}U detector, but they had little effect on those isotopes that had definite fission thresholds (e.g. ^{238}U). This was an important correction so it was measured carefully.

The room return should have little dependence on position, particularly near the center of the room and the neutron source, so it was first measured by obtaining the fission rate of a ^{235}U deposit relative to a ^{238}U deposit as a function of the distance D. Again, the actual dependent variable was the geometry factor, G, which corrected for the departure from a D^2 dependence at small D. Since the previous measurement had shown that the fission rate of ^{238}U had no significant dependence on G, then

$$(C_{235}/C_{238}) = a + bG \qquad (5)$$

Consequently, this measurement was essentially the same as the one described in Section V.A. Measurements over distances between 5 and 18 cm

are illustrated in Fig. 6. A least squares fit gave the ratio of room return fissions to direct fissions for pure ^{235}U as

$$G\ (0.424 \pm 0.012) \times 10^{-3}$$

Although the room return was fairly stable, it could be changed by moving material inside the room and thus could not be relied on to remain constant over long periods of time. Consequently, it was necessary to make frequent measurements of the room return. The above method was too cumbersome and time consuming to be used repeatedly so routine room return measurements were made with a pulsed beam. The beam pulse had a width of 5 μsec and a period of 21 μsec. Neutron yield was reduced by a factor of $> 10^5$ during the beam OFF period. A time spectrum for ^{235}U (Fig. 5) shows the beam pulse sitting on a constant background. It was assumed that the room return fission rate was the same during the beam pulse as it was between the pulses. Measurements were made at a number of distances and they are compared with the results of the first method in Table VI. The agreement is generally good; certainly any difference would have little effect on the cross section ratios. Also the first method does not distinguish between the prompt and slow room return while the second method puts any prompt room return in the main peak and only measures the slower component. Thus the agreement between the two methods indicates that prompt scattering from distant scatterers, already shown to be negligible for ^{238}U, was not a significant effect for ^{235}U.

C. Deposit Thickness, Incident Particle Momentum and Fragment Angular Distribution.

The correction factor is derived to first order in t/R and γ in ref. 5. The factor for the 180 degree fission detector is

(6) $$L_b = 1 + \omega(\pi/2)\ (t/2R + \gamma)$$

For the 0 degree detector it is

(7) $$L_f = 1 + \omega(\pi/2)\ (t/2R + R\gamma^2/2t - \gamma) \qquad t > R\gamma$$
$$L_f = 1 \qquad t < R\gamma$$

where R is the average fragment range, t is the deposit thickness, γ is the ratio of the velocity of the center of mass to the velocity of the fragment in the center of mass system and $\omega(\pi/2)$ is the normalized fragment angular distribution evaluated at $\pi/2$. When measurements are made with both fission detector orientations and averaged, most of the dependence on the incident particle momentum vanishes and the correction to the average of the two measurements is, to first order,

(8) $$L_{av} = 1 + \omega(\pi/2)\ (t/2R + R\gamma^2/4t) \qquad t > R\gamma$$
$$L_{av} = 1 + \omega(\pi/2)\ (t/4R + \gamma/2) \qquad t < R\gamma$$

The average fragment range, R, was determined by two methods. First, there were direct experimental measurements. The specific fission rate, $\mathcal{F}_s$, was measured for a series of deposits with a wide range of thicknesses placed in 180 degree position. Equation (6) shows that when $\mathcal{F}_s$ is normalized to 1.0 the slope will be

$$\frac{-\omega(\pi/2)}{2(1-\gamma\omega(\pi/2))R} .$$

The results of one of these measurements is shown in Fig. 1 of ref. 8. Second, R can be estimated from other experimental range measurements, provided that the composition of the deposit is known. The measurements of Alexander and Gazdik (24) and Niday (25) show that in pure elements

(9) $$R \simeq 0.67\ A^{1/2}$$

where A is the atomic weight. For a compound

(10) $$1/R = \sum_i W_i/R_i$$

where W_i is the weight fraction of element i.

Unfortunately the actual composition of the samples is not always known. The uranium deposits on platinium were fired to 800 ^{o}C and are U_3O_8. The neptunium samples were fired to a similar temperature and are probably NpO_2. The thorium samples were only fired to a little over 600 ^{o}C. Several thorium deposits were weighed, then the amount of thorium present was measured by isotopic dilution. The weights were always $\simeq$ 5 % larger than those estimated from the composition ThO_2. This suggested a stoichiometric formula of the type $ThO_2 \cdot H_2O$. The uranium deposits that were plated by molecular deposition onto steel or molybdenum plates were heated to only about 300 ^{o}C and were probably some type of hydrated uranyl oxide. The composition $UO_4 \cdot H_2O$ was assumed. The plutonium deposits were treated in about the same way. Their composition is unknown, but they were assumed to have the same average fragment range as the molecular plated uranium. A comparison of the measured ranges and those calculated for the assumed compositions is shown in Table VII. The ranges associated with the individual samples are given in Table IV.

In deriving eqs. (6) and (7), the fission deposit was assumed to be a uniform layer on a smooth backing. If the plate is heavily scored, or if the deposit has gathered into clumps or granules the fraction of fission fragments that go undetected will be greater than that estimated from the average thickness. The samples used in these measurements were selected because they appeared to be uniform. An experimental test which has some bearing on sample uniformity is described in the following section.

D. Fission Events Below the Bias Level.

The bias level was set at a point in the flat region between the

alphas and fissions, as shown in Fig. 4, and the spectrum was extended horizonally to zero channel. This extrapolation correction depended on the thickness and, to some degree, orientation of the deposit. For the thinner deposits it was usually a little larger for the 0 degree detector. For thick deposits the correction appeared to be nearly independent of direction. A Monte Carlo simulation of a fission detector pulse height spectrum, shown in Fig. 7, suggests that the horizontal extrapolation is reasonable although there does appear to be some pile-up in the lowest channels.

Fig. 8 shows a plot of the average extrapolation correction vs. the average thickness correction for the samples used. The line is a least squares fit to the ^{232}Th, U and ^{237}Np data only. Most points cluster fairly well about the line and the agreement can be considered fairly good. This is particularly true when it is remembered that the extrapolation correction is a rather imprecise quantity whose size depends on just where the bias level was set. In these measurements no attempt was made to hold the bias levels at a fixed position. Instead the amplifier gains and bias levels were adjusted for each sample. The points furthest from the line are identified in Fig. 8. One of these samples, 238-213, appears to be slightly granular but four of these points are ^{230}Th and ^{239}Pu deposits which have high alpha rates. However, 239-13 which also has a high alpha rate is in very good agreement. This behavior might also be caused by some characteristic of the deposits but the ^{232}Th and ^{242}Pu samples, which have similar deposits, are very near the line. Taken as a whole this comparison indicates that the deposit thickness and extrapolation corrections are reasonably consistent. There are departures but the specific cause is not known. There does seem to be a problem with the ^{230}Th and the ^{239}Pu deposits so the error associated with these samples was increased as described in Section VII.

E. Coincidence Correction.

Since the outputs of the two detector systems were mixed before

going to the multichannel analyzer there was some loss due to accidental coincidences. These events fell into analyzer group 3 and their number was added to the spectra in groups 1 and 2 as indicated by eq. (2). Count rates were never high so the correction was typically < 0.1 %. A few events arrived without their identification signals and were stored in group 0. It was assumed that the loss from a detector was proportional to the count rate so there was no correction to the ratio. Losses of this type were also typically < 0.1 %.

F. Correction for the Minor Isotopes.

This correction is contained in eq. (1) and it was calculated using fission cross sections from ref. (26). It was a little more complicated for the lower-energy measurements where multiple neutron producing reactions in the source made it necessary to carry out an integration over the neutron spectrum, as indicated in Section II.4.5 of ref. (11). However, the 14-MeV generators provided a fairly clean, nearly mono-energetic neutron spectrum so the average energy and average cross sections were used.

VI. MEASUREMENT PROCEDURES.

The determination of a cross section ratio for a pair of samples required at least 6 measurements. The fission detector was placed about 6.5 cm from the neutron source. The chamber was thoroughly flushed and the amplifier gains adjusted so that a few of the pulses reached the amplifier limit. The constant fraction discriminator was adjusted to a point well above the alphas and a time spectrum was recorded to determine the room return correction. When the fission chamber pulse height spectrum was measured the constant fraction discriminator level was set low enough so that it was triggered occasionally by alpha pile-up. The bias level for determining the extrapolation correction was set later on inspection of the spectrum (see Fig. 4). After this adjustment the zero channel on the multichannel analyzer was located using a precision pulser.

Pulse height spectra were recorded for the two fission detectors. The amplifier gain was changed, the discriminator level reset and a second pair of pulse height spectra were recorded. The positions of the samples in the fission chamber were interchanged and the complete process was repeated. The measurement time was long enough to accumulate at least 30,000 counts for each spectrum.

The individual pulse height spectra were corrected for room return, extrapolation to zero channel and coincidences. Their ratio, C_1/C_2, was calculated for each orientation of the samples. The results for the two orientations were combined to give $\overline{(C_1/C_2)}$. This was corrected for prompt neutron scattering and the losses in the deposit, as indicated in eq. (3). Finally, σ_x/σ_r was calculated.

VII. EXPERIMENTAL ERROR.

The sources of experimental error have been examined to provide an indication of the reliability of the experimental results and to properly average the data. Table VIII lists these sources and gives the magnitude range for each component. Correlation information is often imprecise so an effort was made to choose error components in such a way that the reasonable correlations would be either 1.0 or 0. Correlations are not given in Table VIII since the degree of correlation of a particular error will often depend on the context. The sources of error are discussed in greater detail below.

1. Random Errors in $\mathcal{F}_x/\mathcal{F}_r$. These are the statistical counting errors and include any statistical errors associated with the determination of the extrapolation correction and the room return. If a measurement of $\mathcal{F}_x/\mathcal{F}_r$ was made at thermal energies for the determination of N_x/N_r then a similar error applies to that quantity. Experience has shown that when repeated independent measurements aew made using the same pair of samples, the scatter of the results were larger than predicted by the statistical

counting errors. A "non-reproducibility" error was added to account for this.

2. Alpha Count. This includes the counting statistics and all other errors associated with the reproducibility of the alpha count and it was set at 0.3 % for all samples. Since these are ratio measurements, and since all the alpha counting was done in the same counter, the systematic errors largely cancel. Thus the correlation is zero for different samples but 1.0 when the same sample is used.

3. Scattering Correction. The error is 30 % of the correction to the ratio but not less than 0.2 % of the ratio. It is fully correlated for all measurements of a given cross section ratio.

4. Alpha Half-lives. These errors are given in Table IV.

5. Thickness Correction. This is divided into two parts, one associated with the sample and one with the method. The first part is set at 30 % of the correction. For measurements using common samples the correlation is 1.0. The second part was set at 0.3 % of the cross section ratio and was assumed to be fully correlated for all measurements.

6. Extrapolation Correction. The same as the thickness correction.

7. Thermal fission Cross Section Ratios. All thermal measurements were carried over from ref. (11) and the errors are discussed in that report.

8. Isotopic Analysis. If the amount present was at the 1 % level the error to the cross section ratio was placed at 0.4 %. For major isotopes (> 10 %) the error was negligible. There was complete correlation for all samples made from the same material. An exception to this is the ^{234}U content of 235 5-2 and 5-3 where the error was only 0.2 %.

9. Additional Error for ^{230}Th and ^{239}Pu. All measurements using these samples were given an additional fully correlated error equal to one half the additional thickness correction needed to move the data points in Fig. 8 over to the line.

10. Neutron Energy. There was an apparent error in the fission cross section ratio caused by an error in the neutron energy.

(11) $$\Delta R = \left(dR/d\bar{E} \right) \Delta\bar{E}$$

The error in the energy was primarily due to uncertainties in the deuteron beam energy and the distribution of tritium in the titantium layer of the target. The prominent resonance near 100 keV in the $T(d,n)^4He$ excitation function served to restrict the size of $\Delta\bar{E}$. For this report $\Delta\bar{E}$ is assumed to be ± 0.05 MeV and $dR/d\bar{E}$ was obtained from ENDF/B-V (26). The information on ^{230}Th was inadequate so the ΔR for that isotope was assumed to be the same as for $^{232}Th/^{235}U$.

VIII. RESULTS

The ratios of several ^{235}U deposits were measured to test the experimental procedures and to see if there were any serious inconsistencies among the three batches of material used to make these samples. The data were processed by the normal procedures and gave, as the final result, the ratio of the ^{235}U fission cross section in sample 1 to the ^{235}U fission cross section in sample 2. Of course this should be 1.0. The results for the individual measurements are shown below:

	Ratio	Error (%)
U-235 5-2/U-235 SST-5	1.011	1.5
U-235 5-2/U-235-6	1.009	1.4
U-235 5-2/U-235-14	0.999	1.4
Weighted Average	1.006	1.2

The agreement is well within the experimental error.

The results of the individual measurements for the fission cross-section ratios are shown in Table IX. These were averaged using the method described in ref. (27). The weighted averages, errors and χ^2 are shown in Table X. The results of the present work are compared with ENDF/B-V and other recent measurements in Table XI. The experimental results were restricted to the past decade since ENDF/B-V should represent

the trend of the older data. Many of these measurements were made by time-of-flight and white source techniques and the data points are 700-800 keV apart in the 14 MeV region. The 14.74 MeV value was obtained by interpolating linearly between the points on either side of that energy. Most of the monoenergetic measurements were made with the associated particle technique although other methods were also used. The reported energies did not necessarily fall at exactly 14.74 MeV but no correction was made to account for the energy dependence of the cross section ratio. If values at more than one energy were reported then the one nearest to 14.74 MeV was the one entered in the table. Although many of the monoenergetic experiments measured fission cross sections and not cross-section ratios, measurements of the ^{235}U fission cross section by the same method were reported in all cases so the ratios and their errors could be obtained from the data. The error in the ratio was obtained by combining the errors of the two cross section measurements. This may have over-estimated the ratio error since there will be some common systematic error in the cross sections that will not be present in the ratio. The individual ratios are discussed briefly:

$^{230}Th/^{235}U$: The present measurement is over 20 % larger than the ENDF/B-V (26) value but the evaluation of the ^{230}The fission cross section was based on very little experimental data.

$^{232}Th/^{235}U$: The energy of this measurement lies about half-way up the rise associated with the ^{232}Th(n,2nf) threshold so energy determination could be a problem. However, the present cross section ratio lies between the ENDF/B-V evaluation (26) and the measurements of Behrens et al. (36). The agreement is good.

$^{233}U/^{235}U$: The present measurement is about 4 % larger than that of Adamov et al. (31), Carlson and Behrens (34) and ENDF/B-V (26). The earlier measurements of this series (11) below 10 MeV, which used many of the same samples, were about 2 % larger than those of Carlson and Behrens

and about 1.5 % greater than ENDF/B-V.

$^{234}U/^{235}U$: The present work agrees very well with the time-of-flight results of Behrens and Carlson (32) and with ENDF/B-V (26). The monoenergetic measurement of Adamov et al. (31) is nearly 10 % larger but the experimental error is 6 %.

$^{236}U/^{235}U$: The results of Adamov et al. (31) are in good agreement but the error is large. Behrens and Carlson (32) are smaller by about 4 % but this only about one and a half standard deviations. The ENDF/B-V (26) value is smaller but agrees very well.

$^{238}U/^{235}U$: Table XI list six recent measurements (28-32, 37, 39) that lie in a band only 3.2 % wide which includes the ENDF/B-V value (26). An unweighted average gives 0.563 ± 0.007, about 4 % less than the present work. The difference is well over two standard deviations.

$^{237}Np/^{235}U$: The present result is about 8 % less than the ENDF/B-V value. The monoenergetic measurements of Adamov et al. (31) and Arlt et al. (28) are in fairly good agreement while the time-of-flight measurement of Behrens et al. (35) is ≃ 8 % lower. This is qualitatively consistent with the lower energy results (11) where the difference was ≃ 4 %.

$^{239}Pu/^{235}U$: The present result is substantially less than ENDF/B-V (the difference is nearly 8 %) (26). The seven experimental values listed in Table XI (28-31, 34, 38, 39) also tend to be lower. Their total spread is ≃ 8 % but the unweighted average is 1.138 ± 0.015, in very good agreement with the present work.

$^{242}Pu/^{235}U$: The present work is in good agreement with the measurements of Adamov et al. (31), Behrens et al. (33) and with ENDF/B-V (26).

This information is summarized in Fig. 9 which shows a comparison of

the results of this work with other measurements of the past decade as represented by the weighted averages of the data in Table XI. The results shown are all relative to the corresponding ENDF/B-V (26) fission cross section ratios. The agreement between this work and the average of the other experimental values is generally good with the exception of the $^{238}U/^{235}U$ ratio. The large differences between ENDF/B-V and the recent measurements of the $^{237}Np/^{235}U$ and $^{239}Pu/^{235}U$ ratios are evident.

IX. SUMMARY

The fission cross sections of ^{230}Th, ^{232}Th, ^{233}U, ^{234}U, ^{236}U, ^{238}U, ^{237}Np, ^{239}Pu and ^{242}Pu were measured relative to ^{235}U at 14.74 MeV neutron energy and compared to other recent experimental work and to ENDF/B-V (26). If ^{238}U is excluded the agreement with the other data is good. Agreement with ENDF/B-V is at least fair except in the the cases of ^{237}Np and ^{239}Pu where the experimental values are about 8 % lower.

X. REFERENCES

1. J. W. Meadows, Nucl. Sci. Eng., 49, 310 (1972).

2. J. W. Meadows, Nucl. Sci. Eng., 54, 312 (1974).

3. J. W. Meadows, Nucl. Sci. Eng., 58, 255 (1975).

4. J. W. Meadows, "The Fission Cross Sections of Uranium and Plutonium Isotopes Relative to U-235", Proc. NEANDC/NEACRP Specialists Meeting on Fast Neutron Fission Cross Sections of U-233, U-238 and Pu-239, June 28-30, Argonne National Laboratory (1976), ANL-76-90, p. 73.

5. J. W. Meadows, "The Fission Cross Section of ^{239}Pu Relative to ^{235}U from 0.1 to 10 MeV", ANL/NDM-39, Argonne National Laboratory 1976).

6. J. W. Meadows, Nucl. Sci. Eng., 65, 171 (1978).

7. J. W. Meadows, Nucl. Sci. Eng., 68, 360 (1978).

8. J. W. Meadows, "The Fission Cross Section of ^{230}TH and ^{232}Th Relative to ^{235}U", Proc. Intl. Cong. Nuclear Cross Sections for Technology, Knoxville, Tennessee, Oct. 22-26, 1979, NBS Special Publication 594, p. 479, U. S. Bureau of Standards (1980).

9. J. W. Meadows, Nucl. Sci. Eng., 70, 233 (1981).

10. J. W. Meadows, Nucl. Sci. Eng., 85, 271 (1983).

11. J. W. Meadows, "The Fission Cross Sections of Some Thorium, Uranium, Neptunium and Plutonium Isotopes Relative to ^{235}U", ANL/NDM-83, Argonne National Laboratory (1983).

12. Texas Nuclear Generator Model No. 9400, Texas Nuclear Corporation (A subsidiary of Nuclear Chicago Corp.), P. O. Box 0267, Austin, Texas 78756.

13. Safety Light Corporation, 4150A Old Berwick Road, Bloomsburn, Pennsylvania 17815.

14. C. Budtz-Jorgensen and H.-H. Knitter, Nucl. Sci. Eng., 79, 380 (1981).

15. W. P. Poenitz and J. W. Meadows, "^{235}U and ^{239}Pu Sample-Mass Determinations and Intercomparisons", ANL/NDM-84, Argonne National Laboratory (1983).

16. C. Bonnet, P. Hillion and G. Nardin, Nucl. Instr. Methods 54, 321 (1967).

17. P. Burtt, Nucleonics 5, p. 28, Aug. 1949.

18. W. Parker, H. Bildstein and N. Getoff, Nucl. Instr. Methods, 26, 55 (1964).

19. R. Ko, "Electrodeposition of the Actinide Elements", HW-41025, Hanford Atomic Products Report (1956).

20. C. W. Reich, "Actinide Half-Lives as Standards for Nuclear Data Measurements: Current Status", Nuclear Standard Reference Data, International Atomic Energy Agency, Vienna, 1985, p. 390.

21. J. W. Meadows, R. J. Armani, E. L. Callis and A. M. Essling, Phys. Rev. C 22, 750 (1980).

22. "Proposed Recommended List of Trans-Actinium Isotope Decay Data. Part I. Half-Lives", A. Lorenz, editor, INDC(nds)-108/N, IAEA Nuclear Data Section, Vienna (1979).

23. D. L. Smith and J. W. Meadows, "Neutron Inelastic Scattering Studies for Lead-204", ANL/NDM-37, Argonne National Laboratory, Argonne, Illinois 60439 (1977).

24. J. M. Alexander and M. F. Gazdil, Phys. Rev., 120, 874 (1960).

25. J. B. Niday, Phys. Rev., 121, 1471 (1961).

26. "Evaluated Neutron Data File, ENDF/B-V", **ENDF/B Summary Documentation**, compiled by R. Kinsey, ENDF-201, 3rd Edition, Brookhaven National Laboratory (1979).

27. Donald L. Smith, "Covariance Matrices and Applications to the Field of Nuclear Data", ANL/NDM-62, Argonne National Laboratory (1981).

28. R. Arlt, W. Grimm, M. Josch, G. Musiol, H.-G. Ortlepp, G. Pausch, R. Teichner, W. Wagner, I. D. Alkhazov, L. B. Drapschinsky, V. N. Dushin, S. S. Kovalenko, O. I. Kostochkin, K. A. Petrzhak and V. I. Shpakov, "The Application of a Time-Correlated Associated Particle Method for Absolute Cross-Section Measurements of Heavy Nuclides", **Neutron Cross Sections for Technology**, J. L. Fowler, C. H. Johnson and C. D. Bowman, editors, U. S. Department of Commerce (1980), p. 990.

29. M. Cance' and G. Grenier, Nucl. Sci. Eng., 68, 197 (1978).

30. M. Mahdavi, G. F. Knoll and J. C. Robertson, "Measurements of the 14 MeV Fission Cross Sections for ^{235}U and $^{239}Pu^{n}$, Nuclear Data for Science an Technology, K. H. Boeckhoff, ed., D. Riedel Publishing Co. (1983).

31. V. M. Adamov, I. D. Alkhazov, S. E. Gusev, L. B. Drapchinsky, V. N. Dushin, A. V. Fomichev, S. S. Kovalenko, O. I. Kostochkin, L. Z. Malkin, K. A. Petrzhak, L. A. Pleskachevsky, V. I. Shpakov, R. Arlt and G. Musiol, "Absolute Measurements of Induced Fission Cross Sections of

Heavy Nuclides for both ^{252}Cf Fission Neutrons and 14.7 MeV Neutrons", Neutrons Cross Sections for Technology, J. L. Fowler, C. H. Johnson and C. D. Bowman, editors, U. S. Department of Commerce (1980), p. 995.

32. J. W. Behrens and G. W. Carlson, Nucl. Sci. Eng. 63, 250 (1977).

33. J. W. Behrens, R. S. Newbury and J. W. Magana, Nucl. Sci. Eng. 66, 433 (1978).

34. G. W. Carlson and J. W. Behrens, Nucl. Sci. Eng. 66, 205 (1978).

35. J. W. Behrens, J. C. Browne and J. C. Walden, Nucl. Sci. Eng. 80, 393 (1982).

36. J. W. Behrens, J. C. Browne and E. Ables, Nucl. Sci. Eng. 81, 512 (1982).

37. F. C. Difilippo, R. B. Perez, G. de Saussure, D. K. Olsen and R. W. Ingle, Nucl. Sci. Eng. 68, 43 (1978).

38. L. W. Weston and J. H. Todd, Nucl. Sci. Eng. 84, 248 (1983).

39. M. Varnagy and J. Csikai, Nucl. Instr. Methods 196, 465 (1982).

40. R. Arlt, W. Meiling, G. Musiol, H.-G. Ortlepp, R. Teichner, W. Wagner, I. D. Alchazov, O. I. Kostočkin, S. S. Kovalenko, K. A. Petržak, V. I. Spakov, Kereenergie 24, 48 (1981).

Table I. The Isotopic Composition of the Thorium and Neptunium Samples.

	Isotopic Composition (mole %)		
Sample No.	230	232	237
230 - 54 230 - 59	99.516	0.484	____
232 - 30 232 - 31 232 - 34	0.383	99.617	____
237 - 76 237 - 79	____	____	100.000

Table II. The Isotopic Composition of the Uranium Samples.

Sample No.	Isotopic Composition (mole %) 232	233	234	235	236	238
233 - 1002 233 - 1202 233 - 1402	0.8 ppm	99.540	0.184	0.062	0.013	0.203
234 - 3 234 - 4 234 - 5	____	____	99.900	0.064	0.036	< 0.007
234 - 31 234 - 32	____	____	89.950	9.920	0.053	0.075
235 SST-5 235 SST-8	____	____	0.859	93.241	0.332	5.568
235 5 - 2 235 5 - 3	____	____	1.025	98.440	0.437	0.098
235 - 1	____	____	0.028	99.856	0.062	0.054
235 - 6 235 - 10 235 - 14	____	5.127	0.050	94.420	0.307	0.094
236 - 2 236 - 4 236 - 5 236 - 6	____	____	____	0.402	99.593	0.011
236 - 35	____	____	0.015	13.64	86.19	0.16
236 - 36	____	____	0.004	11.00	88.84	0.16
238 - 210 238 - 213	____	____	1.012	2.369	0.132	96.486
238 8 - 2	____	____	0.114	10.840	0.050	88.993
238 - 9 238 - 15	____	10.050	0.022	0.015	____	89.914
238 - 60	____	< 0.6 PPM	____			100.00

Table III. The Isotopic Composition of the Plutonium Samples

	Isotopic Composition (mole %)				
Sample No.	238	239	240	241	242
239 - 13	___	98.944	1.012	0.049	___
239 - 146	___	99.952	0.048	___	___
239 - 267	___	99.952	0.048	___	___
242 - 49	0.007	9.128	0.097	0.099	90.669

Table IV. The Half-Lives and Thermal Fission Cross Sections.

Isotope	Alpha Half-life (years)	$\langle\sigma_F\rangle$ (20°C Maxwellian) (barns)
^{230}Th	$(7.538 \pm .030) \times 10^{4}$ [a]	
^{232}Th	$(1.405 \pm .006) \times 10^{10}$ [b]	
^{233}U	$(1.592 \pm .002) \times 10^{5}$ [c]	526.6 [d]
^{234}U	$(2.457 \pm .003) \times 10^{5}$ [c]	
^{235}U	$(7.037 \pm .007) \times 10^{8}$ [c]	570.4 [d]
^{236}U	$(2.343 \pm .004) \times 10^{7}$ [b]	
^{238}U	$(4.468 \pm .005) \times 10^{9}$ [c]	
^{237}Np	$(2.14 \pm .01) \times 10^{6}$ [c]	
^{239}Pu	$(2.411 \pm .003) \times 10^{4}$ [c]	792.6 [e]
^{240}Pu	$(6.563 \pm .007) \times 10^{3}$ [c]	1060.9 [d]
^{241}Pu (α)	$(6.00 \pm .05) \times 10^{5}$ [c]	
(β)	$(1.44 \pm .01) \times 10^{1}$ [c]	
^{242}Pu	$(3.735 \pm .011) \times 10^{5}$ [c]	

[a] Ref. 21
[b] Ref. 22
[c] Ref. 20
[d] Ref. 26
[e] Ref. 11

Table V. Additional Sample Related Data

Sample #	Av. At. Wt.	Dia. (mm)	Specific Activity (α/sec/μg)	Wt.[a] Element (μg)	Thickness mg Element (mg/cm^2)	Av.Frag. Range (mg/cm^2)	Backing
Th-230-54	230.043	25.4	759.1	771.0	0.152	5.1	0.13 mm Pt
Th-230-59	230.043	25.4	759.1	372.7	0.074	5.1	0.13 mm Pt
Th-232-30	232.030	25.4	2.901	1401	0.276	5.1	0.13 mm Pt
Th-232-31	232.030	25.4	2.901	1407	0.278	5.1	0.13 mm Pt
Th-232-34	232.030	25.4	2.901	2927	0.578	5.1	0.13 mm Pt
U-233-1002	233.058	25.1	355.3	218.2	0.044	4.1	0.13 mm Pt
U-233-1202	233.058	25.2	355.3	255.7	0.051	4.1	0.13 mm Pt
U-233-1402	233.058	24.8	355.3	298.7	0.062	4.1	0.13 mm Pt
U-234-3	234.045	25.4	229.6	298.1	0.059	4.1	0.25 mm ST
U-234-4	234.045	25.1	229.6	359.6	0.073	4.1	0.25 mm ST
U-234-5	234.045	24.6	229.6	419.6	0.088	4.1	0.25 mm ST
U-234-31	234.137	25.0	206.8	189.0	0.038	4.1	0.13 mm ST
U-234-32	234.137	25.0	206.8	362.8	0.074	4.1	0.13 mm ST
U-235-1	235.044	25.4	---b	---b	0.054	4.1	0.13 mm MO
U-235 SST-5	235.200	25.4	2.033	416.8	0.082	4.7	0.25 mm ST
U-235 SST-8	235.200	25.4	2.033	1014	0.199	4.7	0.25 mm ST
U-235 5-2	235.041	24.8	2.436	832.9	0.172	4.1	0.25 mm ST
U-235 5-3	235.041	25.4	2.436	324.2	0.064	5.9	0.13 mm Pt
U-235-6	234.942	25.8	18.47	2860	0.055	4.1	0.13 mm Mo
U-235-10	234.942	27.6	18.47	266.2	0.044	4.1	0.13 mm Mo
U-235-14	234.942	27.6	18.47	357.4	0.060	6.1	0.13 mm Mo
U-236-4	236.056	25.1	2.383	386.0	0.078	4.1	0.25 mm ST
U-236-5	236.056	25.4	2.383	595.0	0.117	4.1	0.25 mm ST
U-236-6	236.056	26.2	2.383	667.5	0.124	4.1	0.25 mm ST
U-236-35	285.924	25.4	2.074	297.5	0.059	4.1	0.13 mm Mo
U-236-36	235.948	25.2	2.135	614.7	0.123	4.1	0.13 mm Mo
U-238-9	237.547	25.2	35.21	383.6	0.077	4.1	0.13 mm Mo
U-238-15	237.892	28.4	11.02	359.7	0.057	4.1	0.13 mm Mo
U-238-60	238.051	25.4	0.01244	1961	0.387	4.1	0.25 mm ST
U-238 8-2	237.716	25.2	---b	---b	0.160	4.1	0.25 mm ST
U-238-210	237.936	25.4	2.303	1180	0.233	5.9	0.13 mm Pt
U-238-213	237.936	25.4	2.303	597.6	0.118	5.9	0.13 mm Pt
Np-237-76	237.048	24.4	26.08	1775	0.350	5.6	0.13 mm Pt
Np-237-79	237.048	25.4	26.08	656.1	0.129	5.6	0.13 mm Pt

Table V. Additional Sample Related Data
(Continued)

Sample #	Av. At. Wt.	Dia. (mm)	Specific Activity (α/sec/μg)	Wt.[a] Element (μg)	Thickness mg Element (mg/cm^2)	Av.Frag. Range (mg/cm^2)	Backing
Pu-239-13	239.077	25.2	2356	281.1	0.056	4.1	0.25 mm ST
Pu-239-146	239.056	25.0	2298	707.2	0.144	4.1	0.25 mm ST
Pu-239-267	239.056	25.0	2298	129.8	0.026	4.1	0.25 mm ST
Pu-242-49	241.054	25.0	384.4	220.7	0.045	4.1	0.13 mm Mo

[a]The specific activities and sample weights were based on isotopic analyses, reported half-lives, and low geometry alpha counting.

[b]The specific activity was not known well enough for accurate sample weight determinations. Fission cross section ratios measured with these samples used mass ratios obtained from relative thermal fission rates.

Table VI. A Comparison of the Room Return for ^{235}U as Measured by the Dependence on the Neutron-Source-Fission-Deposit Distance and by the Pulsed Beam Method.

D (cm)	Geometry Factor	Room Return Fraction: Distance Dependence	Room Return Fraction: Pulsed Beam
5.22	71.1	0.031	0.030
6.12	96.3	0.043	0.043
6.40	105.0	0.046	0.047
6.67	113.8	0.051	0.048
7.11	128.8	0.058	0.060
10.70	2549	0.121	0.114

Table VII. The Measured and Calculated Fission Fragment Ranges.

Element	Assumed Composition	Average Range (mg element/cm^2): measured	Average Range (mg element/cm^2): calculated
U	U_3O_8	____	5.9
	$UO_4 \cdot H_2O$	4.1 ± 05	4.2
	UF_4	4.7 ± 1.0	4.7
Th	$ThO_2 \cdot H_2O$	5.1 ± 03	5.4
Np	NpO_2	5.6 ± 1.4	6.8
Pu	____	(4.1)[a]	___

[a]The range for the Pu deposits was assumed to be the same as for the uranium deposits prepared in a similar way.

Table VIII. Sources and Magnitudes of the Experimental Error.

	Source	Magnitude (%)
1.	Random error in F_x/F_r	
	a. Fission counting statistics b. Extrapolation correction c. Room Return correction d. Reproducibility	0.6 - 0.8
2.	Random error per sample in α-count.	0.3
3.	Half-lives	0.1 - 0.4
4.	Scattering correction	0.2 - 0.7
5.	Thickness correction	
	a. Sample associated	0.2 - 1.5
	b. Method associated	
	For ^{239}Pu and ^{230}Th	0.4 - 1.8
	For other samples	0.3
6.	Extrapolation correction	
	a. Sample associated	0.2 - 1.6
	b. Method associated	0.3
7.	Thermal σ_F ratio	0.5
8.	Isotopic analysis	0.0 - 0.4

Table IX. The Results of the Individual Cross Section Ratio Measurements.

Sample Nos.	Fission Cross Section Ratio			
	R Method 1[a]	Total Error (%)	R Method 2[b]	Total Error (%)
230-54/235 5-2	0.2958	2.2		
230-59/235 SST-5	0.2856	2.1		
230-54/235-14	0.2944	2.2		
232-30/235 5-2	0.1893	2.2		
232-31/235 5-2	0.1915	2.2		
232-34/235 SST-8	0.1931	2.9		
233-1002/235-6	1.150	1.2	1.126	1.2
233-1002/235 SST-5	1.134	1.3		
233-1002/235-10	1.131	1.2	1.141	1.2
233-1202/235 5-2	1.145	1.4		
233-1404/235-14	1.119	1.5	1.124	1.2
234-3/235-14	0.992	1.2		
234-4/235 SST-5	0.989	1.3		
234-4/235 5-3	0.993	1.1		
234-5/235 5-2	1.014	1.4		
234-31/235 SST-5	1.012	1.3		
234-32/235-14	0.991	1.2		
236-4/235-14	0.793	1.3		
236-5/235 SST-5	0.793	1.4		
236-6/235-1	0.792	1.3		
236-6/235 5-2	0.798	1.4		
236-35/235 5-2	0.797	1.4		
236-36/235-1	-----	---	0.781	1.3
238-9/235-6	0.5964	1.3		
238-15/235-14	0.5818	1.3		
238-60/235 SST-8	0.5783	2.3		
238-210/235 5-2	0.5902	1.7		
238-213/235 SST-5	0.5960	1.7		
238 8-2/235 5-2	------	---	0.5834	1.2
237-76/235 SST-5	1.062	2.1		
237-79/235 5-2	1.059	1.6		

Table IX. The Results of the Individual Cross Section Ratio Measurements (Continued).

Sample Nos.	Fission Cross Section Ratio			
	R Method 1[a]	Total Error (%)	R Method 2[b]	Total Error (%)
239-13/235-14	1.159	1.4		
239-146/235 5-2	1.118	2.7		
239-267/235 SST-5	1.153	1.6		
239-267/235 5-2	1.147	1.7	1.145	1.3
242-49/235 SST-5	0.968	1.5		
242-49/235 5-2	0.964	1.4	0.968	1.3

[a] N_x/N_r obtained by low-geometry alpha counting.

[b] N_x/N_r obtained by measuring F_x/F_r in a well thermalized neutron flux.

Table X. The weighted averages of the Data in Table IX.

	Ratio	% err	χ^2	σ_R [a]
230/235	0.2902	1.85	1.37	0.610
232/235	0.1910	1.85	0.26	0.401
233/235	1.132	0.74	1.21	2.378
234/235	0.9982	1.03	1.07	2.097
236/235	0.7907	1.07	0.44	1.661
238/235	0.5866	1.11	0.79	1.232
237/235	1.060	1.42	0.02	2.227
239/235	1.152	1.14	0.45	2.420
242/235	0.9671	1.04	0.06	2.032

[a] The ^{235}U fission cross section used to obtain this column was 2.101 b (ref. 26).

Table XI. A Comparison of this Work with Other Measurements and with ENDF/B-V.

	Energy (MeV)	Ratio	Error (%)	Ratio to this work	Error (%)	Comment and reference
$^{230}Th/^{235}U$	14.74	0.2902	1.9	---	---	This work
	14.74	0.362	---	1.247	---	ENDF/B-V (26)
$^{232}Th/^{235}U$	14.74	0.1910	1.9	---	---	This work
	14.74	0.1952	3.0	1.022	3.4	TOF (36)
	14.74	0.1871	---	0.980	---	ENDF/B-V (26)
$^{233}U/^{235}U$	14.74	1.132	0.7	---	---	This work
	14.7	1.075	2.4	0.950	2.5	AP (31)
	14.74	1.092	2.7	0.965	2.8	TOF (34)
	14.74	1.094	---	0.966	---	ENDF/B-V (26)
$^{234}U/^{235}U$	14.74	0.998	1.0	---	---	This work
	14.7	0.911	6.0	0.913	6.0	AP (31)
	14.74	1.025	2.7	1.027	2.8	TOF (32)
	14.74	1.006	---	1.008	---	ENDF/B-V (26)
$^{236}U/^{235}U$	14.74	0.791	1.1	---	---	This work
	14.7	0.773	5.1	0.977	5.2	AP (31)
	14.74	0.823	2.5	1.040	2.6	TOF (32)
	14.74	0.812	---	1.026	---	ENDF/B-V (26)
$^{238}U/^{235}U$	14.74	0.587	1.1	---	---	This work
	14.7	0.562	2.5	0.957	2.6	AP (31)
	14.7	0.559	2.1	0.952	2.3	AP (28)
	14.7	0.557	3.0	0.949	3.1	AP (29)
	14.74	0.563	1.0	0.959	1.4	TOF (37)
	14.7	0.575	5.7	0.980	5.8	(39)
	14.74	0.570	1.8	0.971	2.0	TOF (32)
	14.74	0.568	---	0.968	---	ENDF/B-V (26)
$^{237}Np/^{235}U$	14.74	1.060	1.4	---	---	This work
	14.7	1.094	2.6	1.032	2.9	AP (31)
	14.7	1.068	1.6	1.008	2.1	AP (28)
	14.8	1.133	5.1	1.069	5.3	(39)
	14.74	0.983	2.7	0.927	3.0	TOF (35)
	14.74	1.148	---	1.083	---	ENDF/B-V (26)

Table XI. A Comparison of This Work With Other Measurements and With ENDF/B-V (Continued).

	Energy (MeV)	Ratio	Error (%)	Ratio to this work	Error (%)	Comment and reference
$^{239}Pu/^{235}U$	14.74	1.152	1.1	---	---	This work
	14.7	1.195	2.5	1.037	2.6	AP (31)
	14.7	1.148	1.5	0.996	1.8	AP (28)
	14.7	1.110	3.0	0.964	3.1	AP (29)
	14.63	1.179	2.4	1.023	2.5	(30)
	14.74	1.106	2.2	0.960	2.4	TOF (34)
	14.74	1.106	2.4	0.960	2.6	TOF (38)
	14.7	1.124	6.1	1.021	6.2	(39)
	14.74	1.239	---	1.076	---	ENDF/B-V(26)
$^{242}Pu/^{235}U$	14.74	0.966	1.0	---	---	This work
	14.74	0.978	2.5	1.012	2.8	AP (31)
	14.74	0.959	2.2	0.993	2.5	TOF (33)
	14.74	0.958	---	0.992	---	ENDF/B-V(26)

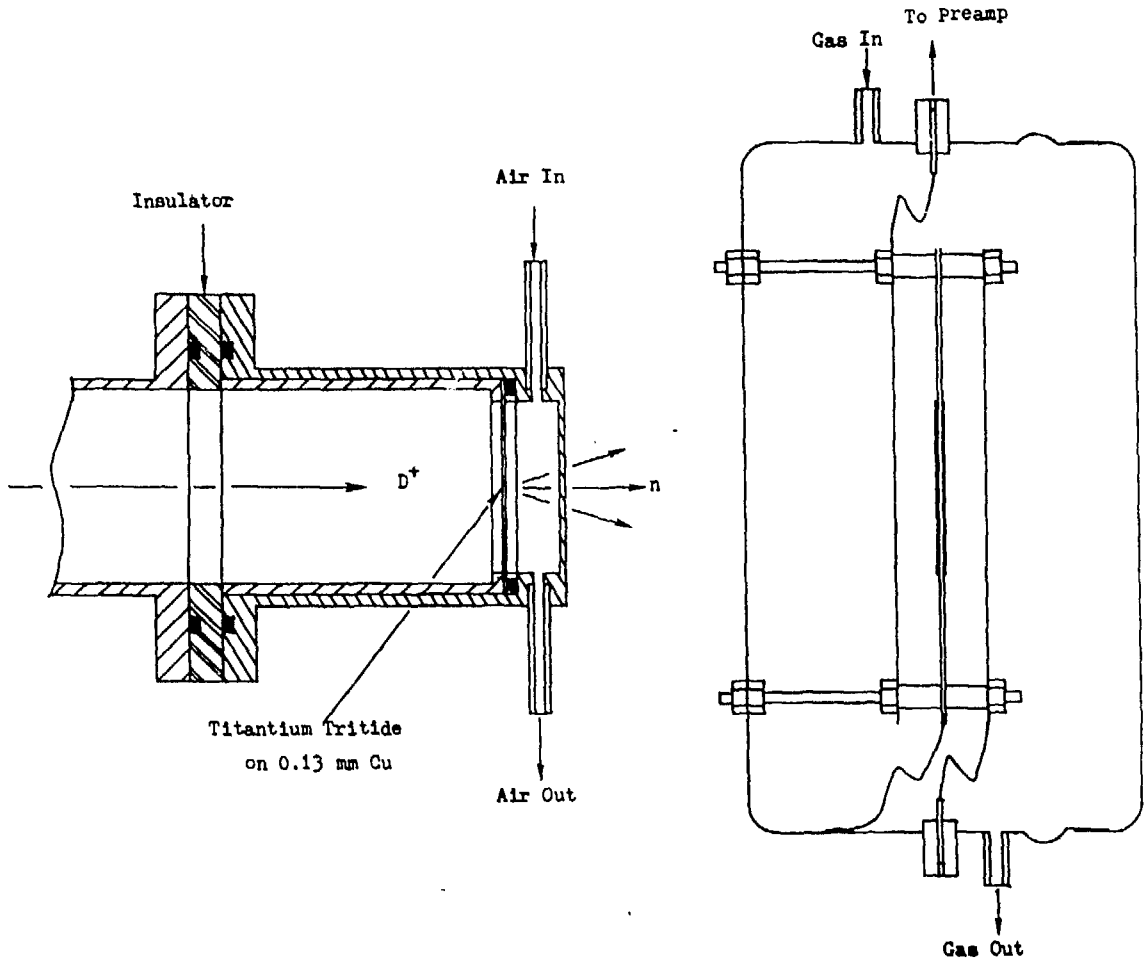

Figure 1. A schematic diagram of the titantium tritide target assembly and the fission detector. The apparatus is drawn to scale with a neutron-source to fission-deposit distance of 6.1 cm.

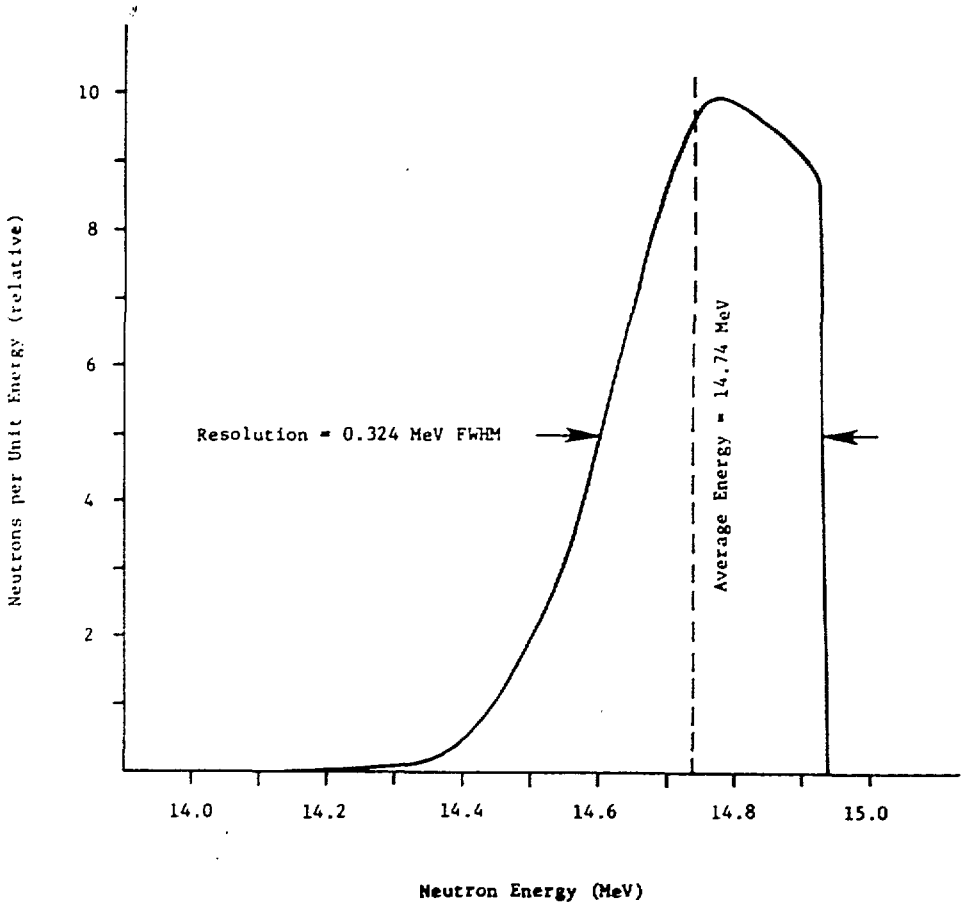

Figure 2. The neutron energy spectrum incident on a 2.54 cm dia. sample 6.5 cm from the neutron source.

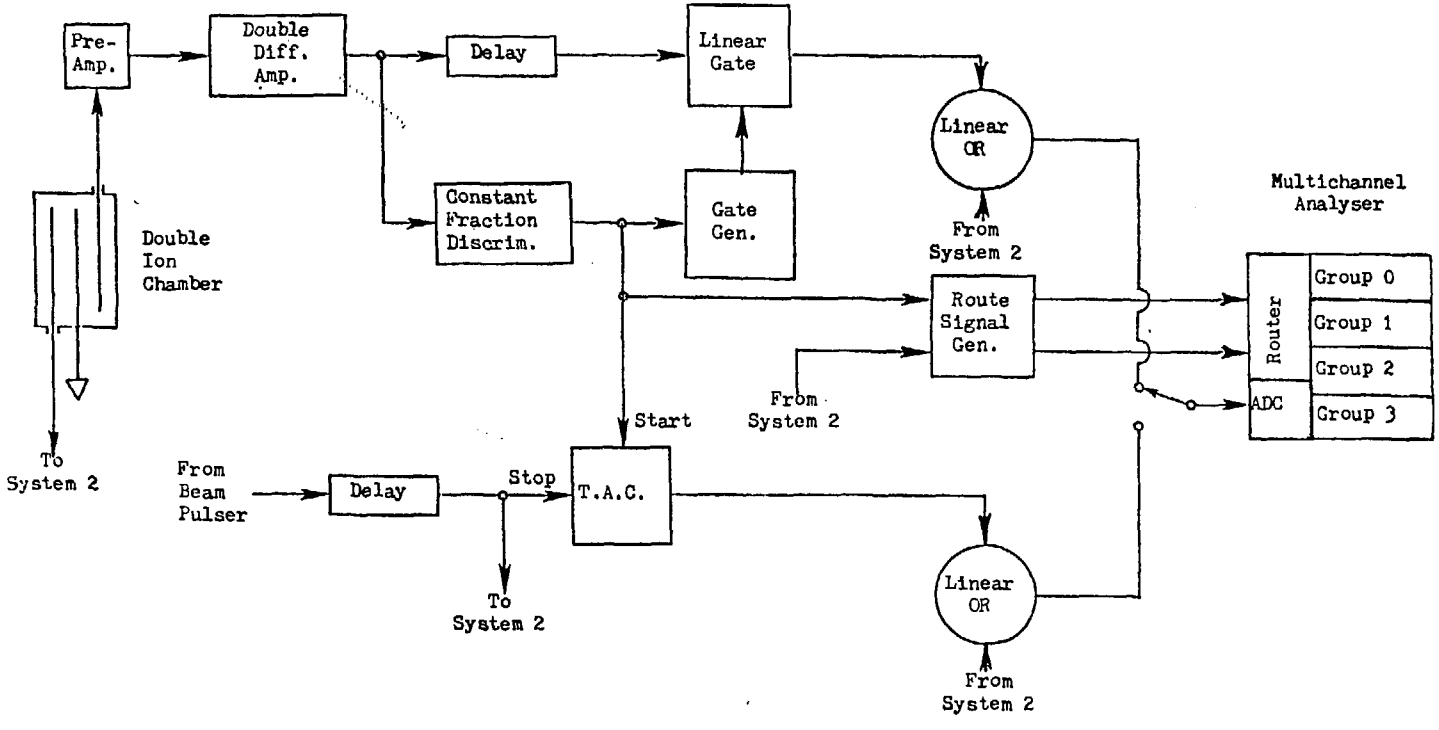

Figure 3. A block diagram of the electronics used in the 14 MeV fission cross section ratio measurements. The complete apparatus consists of two similar electronic systems. Only one is shown in the diagram.

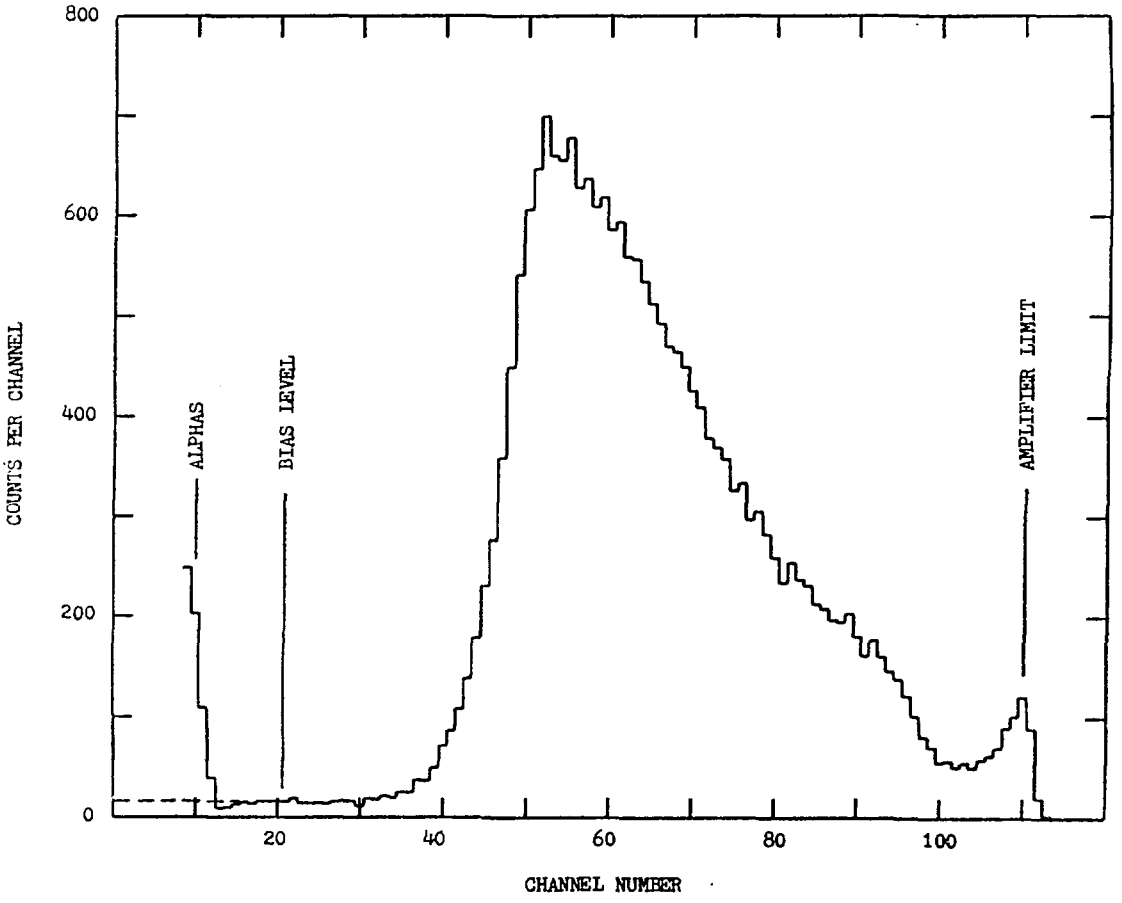

Figure 4. The pulse-height spectrum from the fission chamber for a ^{235}U sample with 0.15 mg U/cm^2.

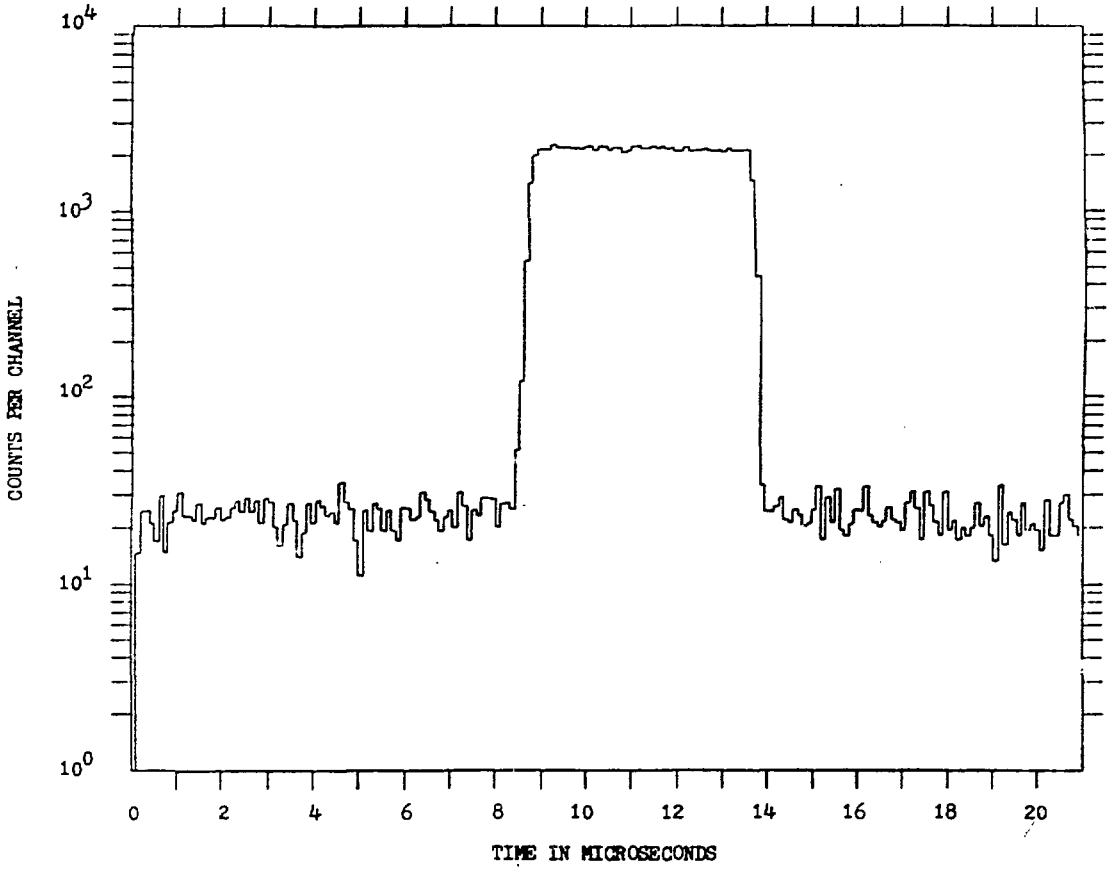

Figure 5. A typical time distribution for ^{235}U. The width of the deuteron beam pulse was 5 μsec.

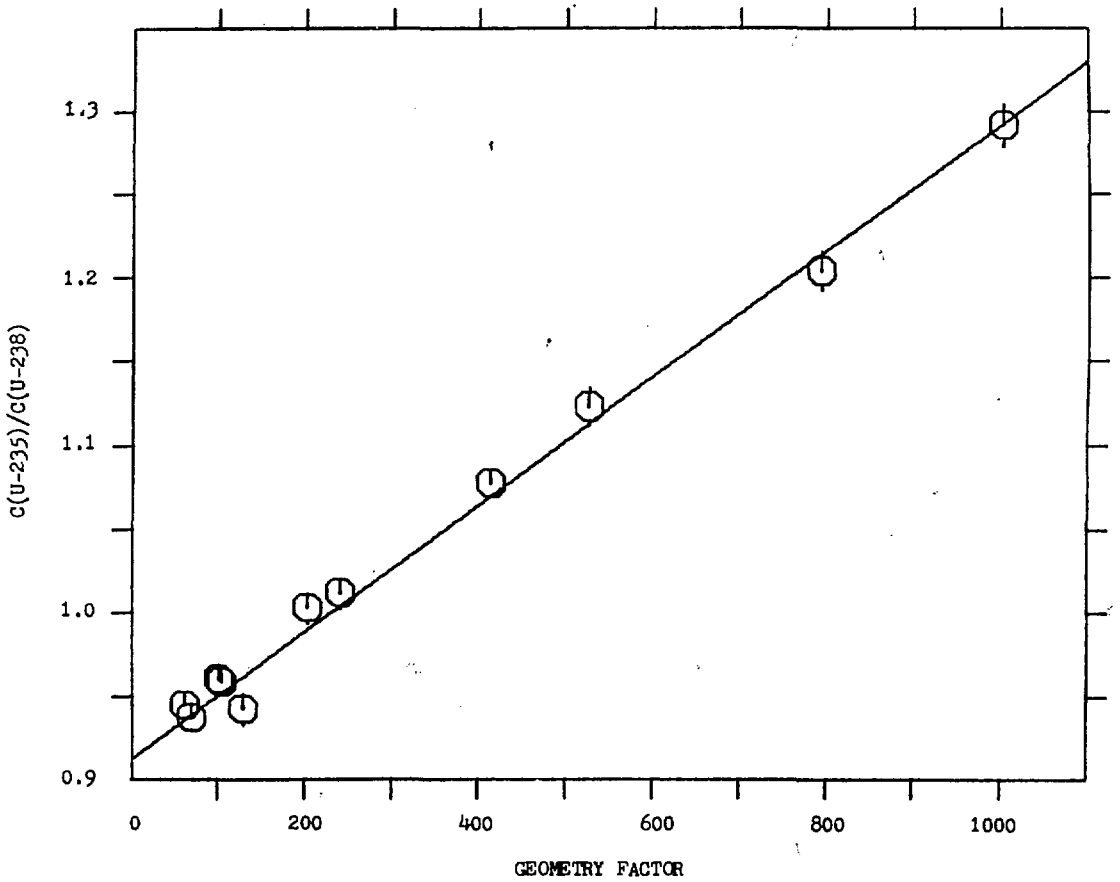

Figure 6. The dependence of the number of ^{235}U fissions relative to the number of ^{238}U fissions on the ^{235}U geometry factor. The data was corrected for scattering from the target and fission chamber structures and for the difference in the geometry factors of the two samples.

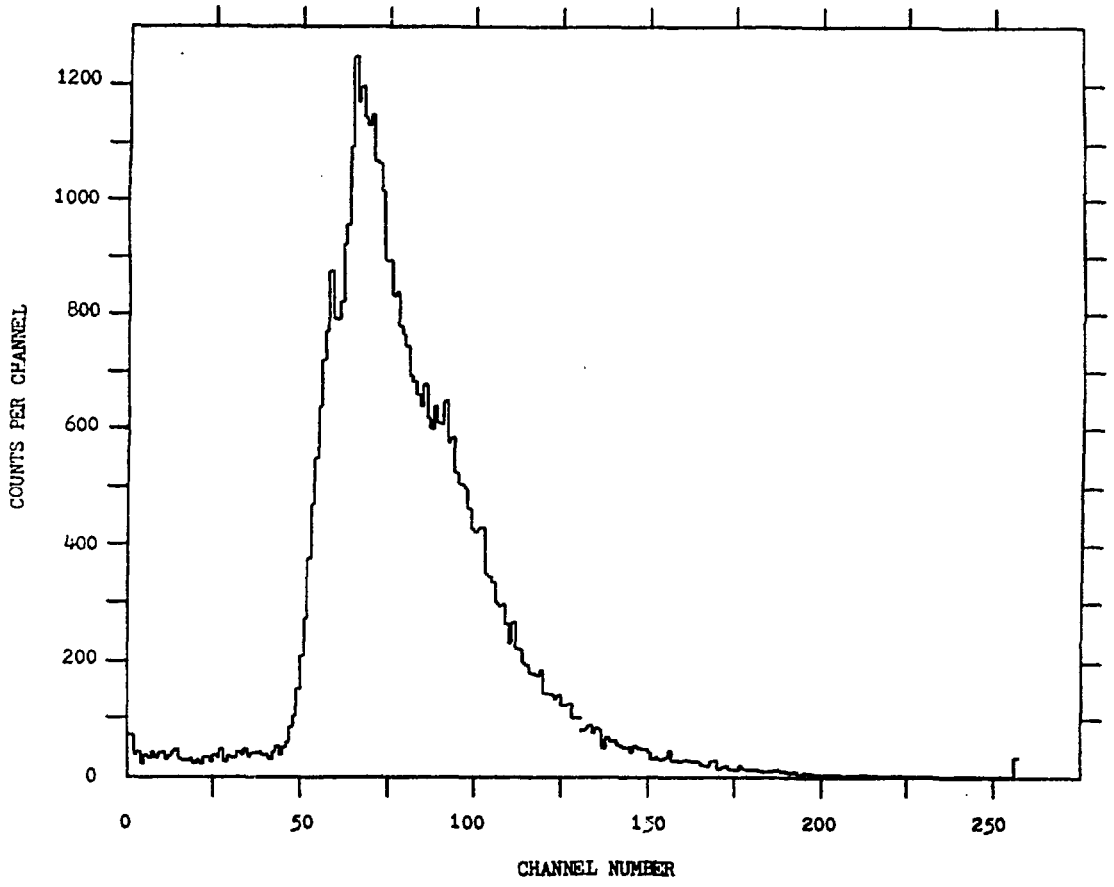

Figure 7. A Monte Carlo simulation of the fission chamber pulse height distribution showing that a flat extrapolation to zero channel is reasonable.

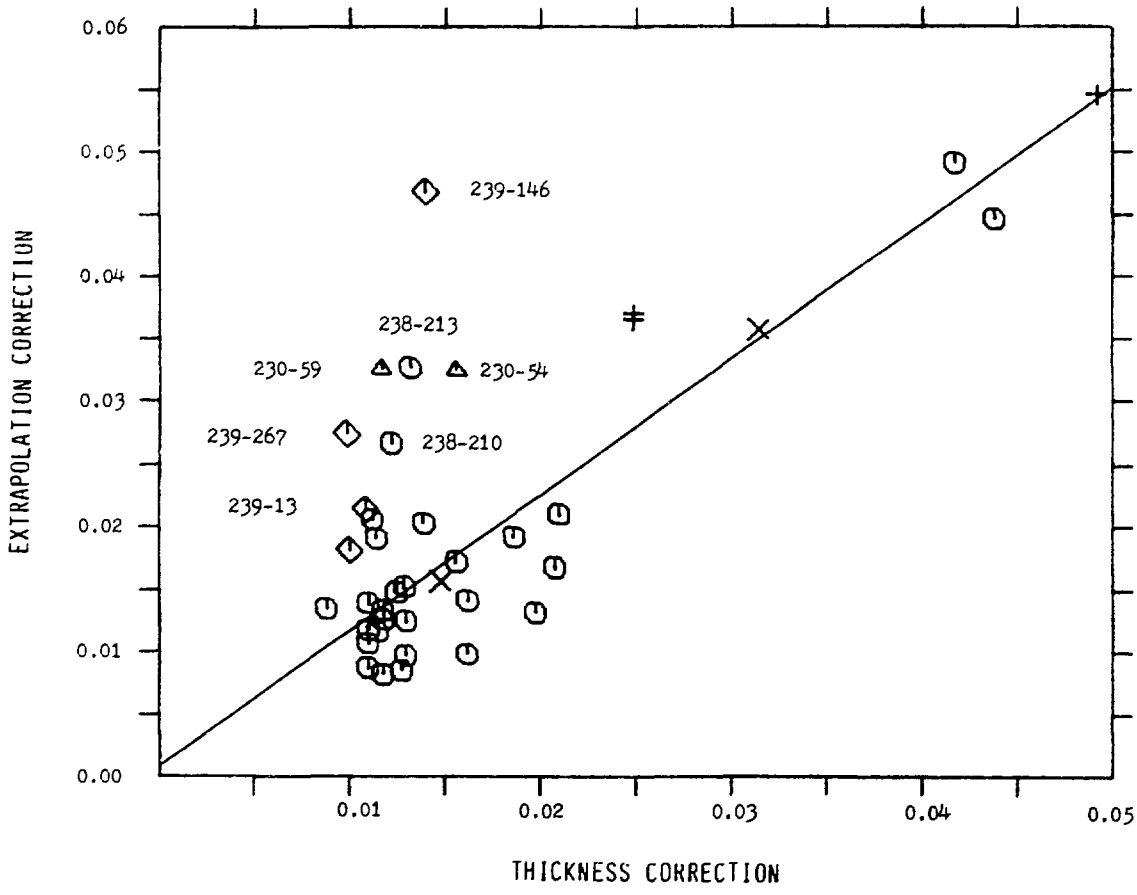

Figure 8. The relation between the extrapolation correction and the deposit thickness correction. The symbols represent: ^{230}Th(△); ^{232}Th(+); all U deposits (O); ^{237}Np(x); all Pu deposits (◇). The individual points that are identified on the plot are discussed in Section V.D.

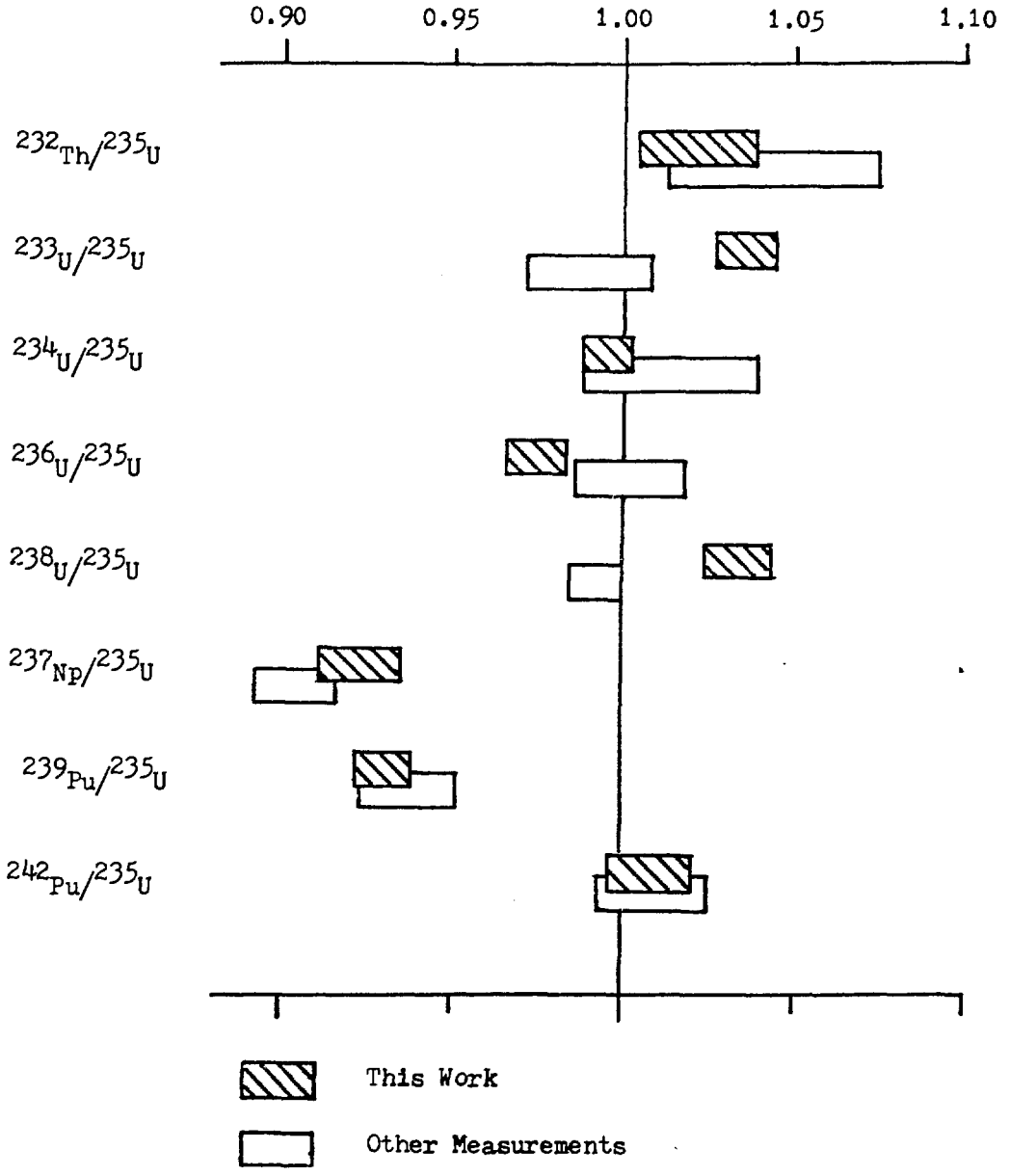

Figure 9. A comparison of the results of this work with other data as represented by the weighted average of the other measurements listed in Table XI. All results have been divided by the corresponding ENDF/B-V fission-cross-section-ratio.